LONG-TERM ELECTROCHEMICAL CRITERIA FOR CREVICE CORROSION IN CONCENTRATED CHLORIDE SOLUTIONS

T. AHN,[1] H. JUNG,[2] P. SHUKLA,[2] AND X. HE [2]

[1]U.S. Nuclear Regulatory Commission, Washington, DC
[2]Center for Nuclear Waste Regulatory Analyses, San Antonio, TX

ABSTRACT

Crevice corrosion is the predominant mode of localized corrosion of Alloy 22 in concentrated chloride solutions at near-boiling temperatures. A literature review was performed to assess the electrochemical criteria for the initiation of crevice corrosion in forecasting the long-term lifetime of the waste package in nuclear waste management. Specifically, this review presents (i) environments (e.g., solution chemistry and electrical polarized condition) and crevice corrosion initiation criteria, (ii) data and models for Alloy 22 crevice corrosion, and (iii) induction times for crevice corrosion initiation. Without externally applied current (i.e., at the open-circuit corrosion potential), initiation of crevice corrosion could be more difficult. In the event of no external current being applied, crevice corrosion may not be initiated and sustained until the corrosion potential reaches a breakdown potential. The breakdown potential is typically more anodic than the repassivation potential. Also, models for the induction time for localized corrosion (i.e., crevice corrosion and pitting corrosion) are evaluated to assess whether laboratory tests can be used to forecast the potential for crevice corrosion development over very long periods of time. The initiation time for crevice corrosion measured in laboratory time periods appears to scale appropriately for extrapolation to very long periods of time.

INTRODUCTION

Crevice corrosion is the predominant mode of localized corrosion of Alloy 22 in concentrated chloride solutions at near-boiling temperatures. The objective of this work is to review relevant literature data on the electrochemical criteria for the initiation of stable crevice corrosion in bulk or thin-film solutions. Although the review is primarily relevant to Alloy 22 in chloride environments at near boiling temperature, it is generally applicable in other systems. The review results are discussed with respect to using the criteria in forecasting the long-term (e.g., many thousand years) lifetime of the waste package in nuclear waste management. When the corrosion potential reaches above the breakdown potential, the literature suggests that protective passive oxide film formed on the metal surface is destabilized, causing localized corrosion or transpassive dissolution without delaying time. When the corrosion potential is lowered below the repassivation potential, the destabilized passive oxide film becomes restabilized and the film persists for a very long time. The breakdown potential is typically higher than or equal to the repassivation potential. However, this general understanding of the breakdown potential

and the repassivation potential is based on the models and data under externally applied current conditions. Under the natural open-circuit conditions, the breakdown potential and repassivation potentials are not well defined. This work discusses the electrochemical criteria, mainly breakdown potential, for the initiation of stable crevice corrosion under open-circuit conditions. Traditionally the breakdown potential is obtained under either potentiostatic or potentiodynamic conditions, as discussed in the literature. In addition to this traditionally defined breakdown potential, this paper discusses the breakdown potential under open-circuit conditions, which is expected to be lower than that under either potentiostatic or potentiodynamic conditions . For comparison purposes, the traditional criteria of repassivation potential obtained under potentiostatic/potentiodynamic controlled conditions (e.g., at $2x10^{-6}$ A/cm^2 [1.3×10^{-5} A/in^2]) are also considered. To obtain the long-term behavior of the initiation criteria for stable crevice corrosion, two types of induction time for the crevice corrosion are reviewed and evaluated. The first induction time is the time to reach a steady-state chemistry, pH and potential inside the crevice. The second induction time is the time to break down the passive film inside the crevice, potentially forming pits based on the point defect model (PDM).[1] If these induction times are short and detectable in the laboratory time scale, it may be possible to understand the long-term behavior of the initiation times for stable crevice corrosion because further long-term latent initiation may not happen. To understand the initiation criteria and its long-term behavior, this paper presents specifically (i) environments and crevice corrosion initiation criteria, (ii) data and models for Alloy 22 crevice corrosion, and (iii) induction times for crevice corrosion initiation.

ENVIRONMENTS AND CREVICE CORROSION INITIATION CRITERIA

The environments needed for crevice corrosion initiation pertain to mainly solution chemistry, temperature, pH and electric polarization condition. In this paper, the concentrated chloride solutions at near-boiling temperatures are primarily considered. The pH covers neutral, acidic and slightly basic ranges. Some oxyanions such as nitrates, carbonates and sulfates are also considered. Experimental studies have shown that higher ratios of the chloride concentration to the concentrations of oxyanions promote crevice corrosion and lower ratios inhibit crevice corrosion.[2] The effect of dominant cations of chloride solutions such as sodium, potassium, calcium and magnesium are also considered.

In the system performance assessment (PA) of nuclear waste management, the initiation criteria of stable crevice corrosion is often adopted on a conservative basis of waste package failure criteria.[3] Once the initiation criteria are met under given external environmental conditions at a time, the Alloy 22 waste package is assumed to fail because crevice corrosion (mainly in a form of pits inside crevice) propagates through the thickness. The propagation of crevice corrosion is assumed to be rapid compared with long-term geological times, once the crevice corrosion is initiated given the appropriate environmental (along with Alloy 22 metallurgical) conditions. Therefore, under this conservative PA assumption, there is no existing propagating crevice corrosion

(mainly with pits) when an Alloy 22 waste package sees a new environment at a different time. The assessment of the crevice corrosion initiation at a different time considers only Alloy 22 waste packages without existing crevice corrosion under propagation.

The initiation criteria could be assessed in further simplified ways if other conservative assumptions were adopted in the PA. For example, other conservative assumptions may include that tight crevices always exist or a certain portion of solutions are always aggressive. In this regard, we assume that the tight crevice gap with an appreciable contact area (or crevice depth) occurs by the contact of Alloy 22 with any type of crevice former. The ratio of the crevice gap to contact area is conservatively assumed to be sufficiently large to initiate crevice corrosion, given aggressive external environmental conditions and/or metallurgical conditions. Detailed knowledge about the fate of the initiated stable crevice corrosion over a long-period of time is not necessary in a conservative PA. Such knowledge may pertain to new environments inside the crevice under crevice corrosion propagation, including salt formation, hydrolysis, pH drop, potential distribution, and volume of crevice solution, in addition to tightness of crevice.[4-11] However, the effective stable initiation conditions (e.g., corrosion potential for the initiation), could exclude to consider short-term transient stifling or repassivation after a transient intiation. Finally, the discussion here assumes that the metallurgical conditions are mill-annealed, unless otherwise specified.

DATA AND MODELS FOR ALLOY 22 CREVICE CORROSION

Crevice Corrosion under Potentiostatic Conditions

Szklarska-Smialowska presented a general concept of a potentiostatic electrochemical criteria for localized corrosion.[12] Although this concept was for pitting corrosion, it could be equally applied to crevice corrosion because the nature of occluded concentration cell is similar and pitting is accompanied in the crevice. Figure 1 shows different stages of localized corrosion Fe-1Cr single crystal in 0.4 N NaCl + 0.7 N Na_2SO_4 as an example case. The number of pits is plotted for various applied potentials.

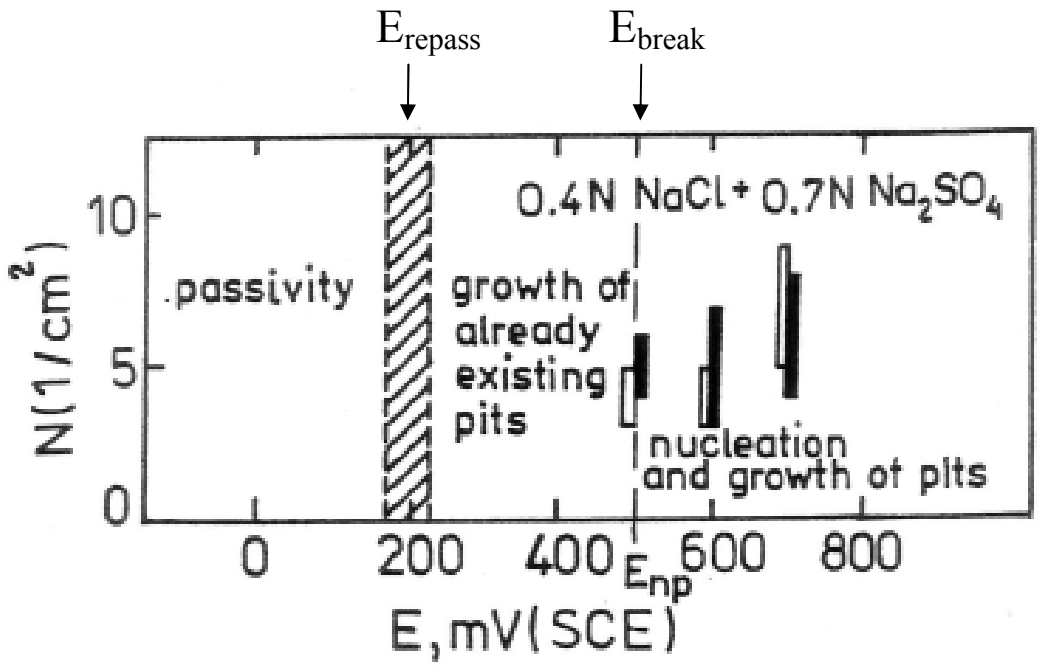

Figure 1. Example of Different Stages of Localized Corrosion
Number of pits (stationary value) vs. potential for (110) and (111) planes of Fe-1Cr single crystals. E_{np} is potential of pit nucleation (equivalent to breakdown potential, E_{break}). The slashed band around 200 mV (saturated calomel electrode, SCE) indicates repassivation potential, E_{repass}.[12] [permission by NACE]

Figure 1 suggests that localized corrosion as pitting could occur in various stages depending on the applied potential:

(i) $E_{corr} < E_{repass}$: no localized corrosion initiation
(ii) $E_{repass} < E_{corr} < E_{break}$: propagation of existing localized corrosion pits
(iii) $E_{corr} > E_{break}$: localized corrosion initiation in the form of pitting

where E_{corr}, E_{break}, and E_{repass} denote the corrosion potential, breakdown potential, and repassivation potential, respectively. The ASM Handbook also presents a similar electrochemical criterion for localized corrosion.[13] For metals that have good resistance to pitting, the second stage, (ii), will not initiate/propagate pitting corrosion .[13]

For nickel-based alloys, Alloy 825, 625 and 22, Dunn, et al.[2] measured the initiation times for the crevice corrosion in 5.5 M NaCl solution at 100 °C. Dunn, et al.[2] measured the initiation times under potentiostatic conditions. The initiation time gradually increased as the applied potential lowered toward the repassivation potential. This result indicates that the repassivation potential is a long-term threshold potential for the initiation of crevice corrosion. They also presented breakdown potentials for crevice

corrosion under cyclic potentiodynamic polarization conditions. For Alloy 22, the crevice repassivation potential, E_{rcrev} (equivalent to E_{repass} in Figure 1), was – 145 mV (SCE). The breakdown potential E_{break}, which is also often denoted as $E_{crev,}$, was 640 mV (SCE). The crevice corrosion instantly initiated at the breakdown potential. The crevice corrosion is not expected to be initiated when the corrosion potential is below E_{rcrev}. Contrary to Figure 1, crevice corrosion was newly initiated at the corrosion potential between E_{crev} and E_{rcrev} after prolonged times.

Crevice Corrosion under Free Open-circuit Corrosion Conditions

He and Dunn[14] monitored current densities and potentials using the single crevice assembly for an Alloy 22 cylindrical specimen galvanically coupled to a large Alloy 22 plate in 5 M NaCl solution with the addition of 2×10^{-4} M $CuCl_2$ at 95 °C [203 °F]. $CuCl_2$ was added to increase the value of corrosion potential. The initiation conditions were obtained without applying continuously external current as used in the potentiostatic method. The Alloy 22 cylindrical specimen was galvanically coupled to Alloy 22 through a zero resistance ammeter and a volt meter to measure the potential of the galvanic couple against the reference SCE.

Figure 2 shows the measured current density and the potential. By adding $CuCl_2$, the current density and potential increased to 1×10^{-4} A/cm^2 [6.5×10^{-4} A/in^2] and 429 mV (SCE), respectively. Potentials are compared with Dunn, et al.[2] where the test conditions were nearly identical except the presence of the oxidizer. The initial corrosion potential present in Figure 2 prior to initiation appears to be in the range of the breakdown potential, because the current density represents the passivity breakdown.[15] This potential is also close to 640 mV (SCE) that seems to be the breakdown potential, and well above the repassivation potential of -145 mV (SCE). If the rates of potential scanning were decreased, the presumable breakdown potential, 640 mV (SCE), could be decreased under potentiostatic conditions.[7] Currently, the breakdown potential for crevice corrosion has not been well defined, especially under open-circuit conditions. Also, the uncertainty range of repassivation potential is relatively large.[2] The crevice corrosion was initiated by adding the oxidizer as shown in Figure 2. The corrosion potential decreased as the crevice chemistry evolved. However, after 8.5 days, the corrosion potential increased to 400 mV (SCE) and still repassivation occurred. Thus, the crevice corrosion was not sustained at the potential well above the repassivation potential, even considering the uncertainties of repassivation potential. It is expected that the crevice corrosion is not even initiated at potentials below 400 mV (SCE).

Based on observations mentioned above, it appears that the crevice corrosion will not be sustained with time under free corroding conditions. With time, the outer cathode may have thicker and crystallographically closer to perfect passive film, decreasing electrochemical reaction rates of cathode reactions. Therefore, the cathode site outside the crevice will not be able to support the pits growing inside the crevice. In addition, the crevice gaps will widen as corrosion progresses. As a consequence of these changes, the electric charge transfer between the cathode and the anode (inside the crevice) could decrease. At a later time, as shown in Figure 2, the current density can drop and the

potential goes up accordingly, resulting in sustaining the repassivation of the crevice corrosion.

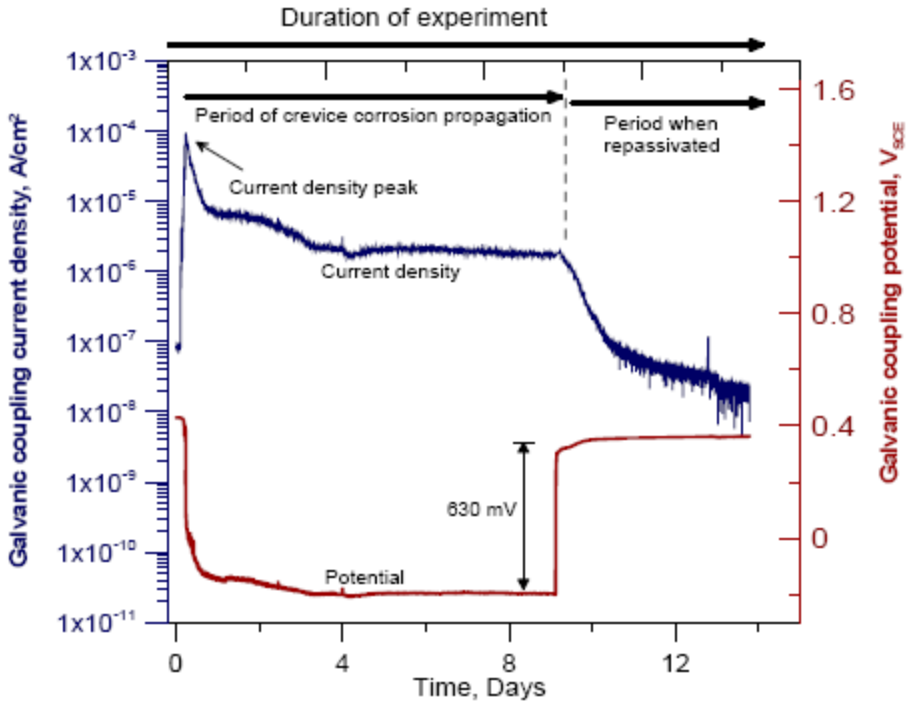

Figure 2. Measured Current Density and Potential Using the Single Crevice Assembly for an Alloy 22 Cylindrical Specimen Galvanically Coupled to a Large Alloy 22 Plate in 5 M NaCl Solution with the Addition of 2 x 10^{-4} M $CuCl_2$ at 95 ºC [203 ºF], mV(SCE)[14]

After the test in Figure 2, the damage of Alloy 22 was characterized. Initially, the total crevice area was corroded. Gradually, the corrosion propagation was localized to pits inside the crevice area. The pit density decreased gradually. In the end, only a few pits of the size 10 – 100 micrometer [(4 – 39) x 10^{-3} inch] were active, and eventually the total crevice area was completely repassivated. A sample, however, showed a single corroded site that persisted and grew to a greater depth than the surrounding area. This type of exception that the pit persisted and grew could be due to metallurgical variations in the crevice. In the similar tests with multiple micro crevice assembly, the potential response was similar and the samples were repassivated.

In another study, Dunn, et al.[2] conducted similar open-circuit crevice corrosion tests for Alloy 22 in 5 M NaCl. They performed tests by galvanically coupling an Alloy 22 crevice specimen to an Alloy 22 plate. With an addition of $CuCl_2$ at 100 °C [212 °F], the initial potential of the couple was 260 mV (SCE), and the current density was in the passive state. No crevice corrosion was initiated for about 4 days. With an increased concentration of $CuCl_2$ at 100 °C [212 °F], the corrosion potential increased to 410 mV (SCE), and the crevice corrosion was initiated.

Figure 3 shows the cyclic polarization curve of Alloy 22 creviced samples (KE0272) after being immersed in 18 M $CaCl_2$ + 0.9 M $Ca(NO_3)_2$ at 155 °C [311°F] for 20 months .[15] The breakdown potential of Alloy 22 after 20 months was near 520 mV (Ag/AgCl), and, the same authors noticed a similar range of breakdown potentials after the 588-day immersion test, which ranged from 547 to 690 mV. For the same samples, the repassivation potentials ranged from 31 to 35 mV. As seen in Figure 4, Rodriguez, et al.[15] also measured the open-circuit potential of creviced Alloy 22 in 18 M $CaCl_2$ + 0.9 M $Ca(NO_3)_2$ at 155 °C [311°F] for 588 days. The corrosion potential, E_{corr}, showed oscillations of up to 600 mV (Ag/AgCl) during the entire immersion period. At this ratio of chlorides to nitrates, crevice corrosion was expected to occur. These oscillations were due to pitting corrosion development outside the crevice. There was no crevice corrosion inside the crevice. Because pitting corrosion was active outside the crevice, the electrochemical cell for crevice corrosion may not have formed, and most of the excess cathode current generated due to oxygen reduction reaction was to be used for supporting pit growth outside the crevice. As the bare metal surface is exposed in the pits, the corrosion potential drops until the pits become repassivated at a potential above the repassivation potential. The corrosion potential goes up again continuously to the breakdown potential. This potential shift repeats, resulting in the oscillation of the corrosion potential. In four other cases (including solution heat treatments) of 18 M $CaCl_2$ + 0.9 M $Ca(NO_3)_2$ (KE0242 to KE0245 in Rodriguez, et al.[15]), pitting was observed outside the crevice in only one case. This suggests that pitting corrosion occurs only when the corrosion potential reaches at or above the breakdown potential. The averaged corrosion potentials of the test samples of KE0272 and KE0242 to KE0245 increased with time. As observed in the initiation of localized corrosion under potentiostatic controlled conditions in this range of potentials, the long time for initiating pitting or crevice corrosion was not noticed under free corroding conditions.

For the tests done in 18 M $CaCl_2$ + 9 M $Ca(NO_3)_2$ solution with ten times of 0.9 M nitrates, no pitting or crevice corrosion was observed for all samples, as expected at the low ratio of chlorides to nitrates. The corrosion potentials were less than the repassivation potential and the breakdown potential. The average corrosion potential decreased with time. The corrosion potential oscillated in this solution too, but the frequency and the amplitude of the oscillation were less than the cases of 0.9 M nitrates. The cause for the oscillation appears to be due to generation and dying of metastable small sized pits.

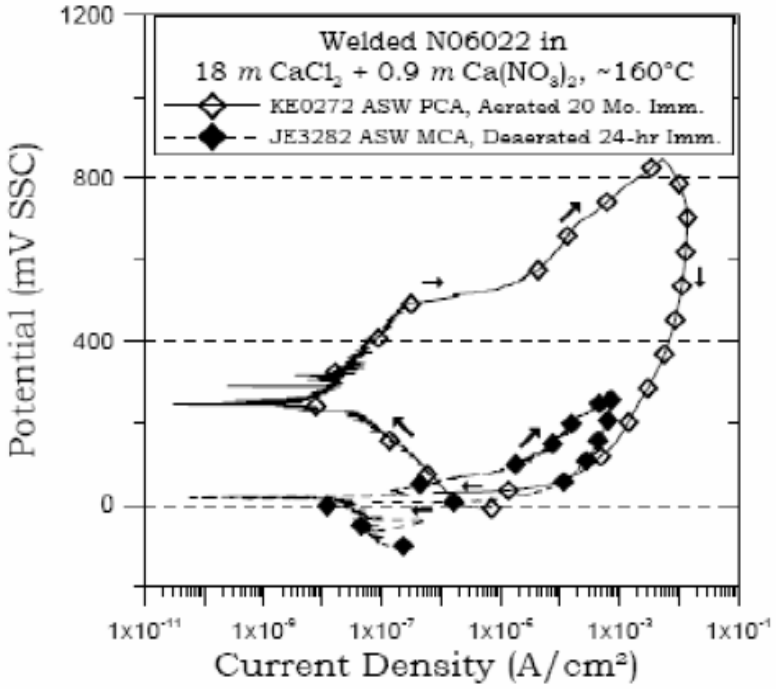

Figure 3. Cyclic Potentiodynamic Polarization for Alloy 22 in 18 M $CaCl_2$ + 0.9 m$Ca(NO_3)_2$, $[NO^3\text{-}]/[Cl^-]$ = 0.05 at ~ 160 ºC [320 ºF] Comparing Short and Long Term Immersion. Short Term Data Is At 160 ºC [320 ºF], Long Term at 155 ºC [311 ºF] [Rodriguez, et al.,[15] permission by NACE]

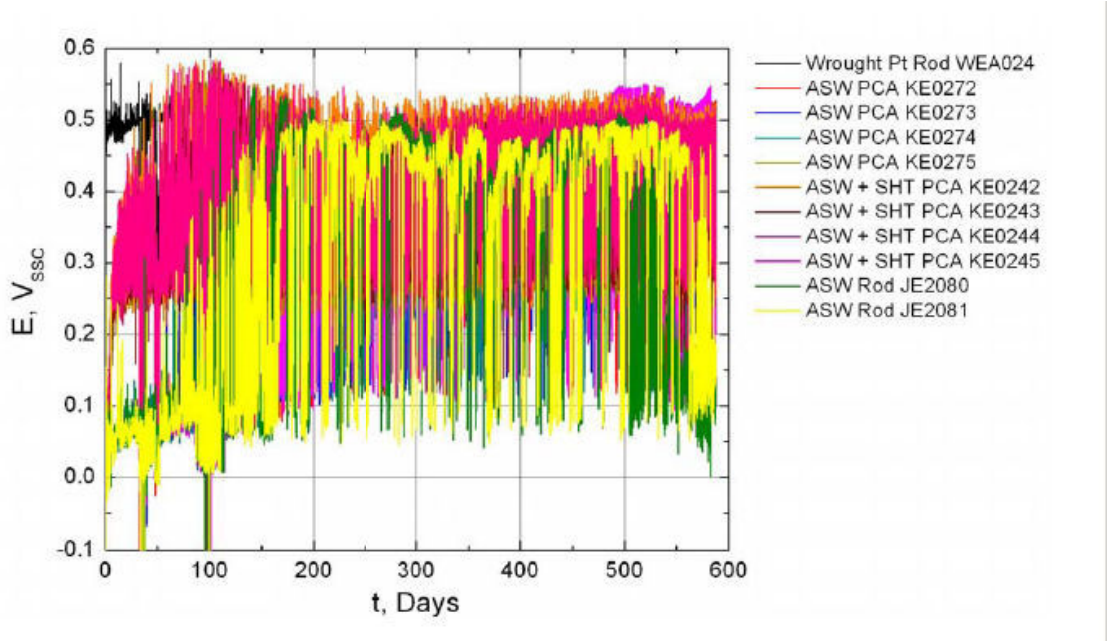

Figure 4. Corrosion Potential as a Function of Immersion Days for Alloy 22 Specimens in 18 M $CaCl_2$ + 0.9 M $Ca(NO_3)_2$ [Rodriguez, et al.,[15] permission by NACE]

In more severe environments, He and Dunn[14] performed galvanically coupled open-circuit tests of creviced Alloy 22 in 4 M $MgCl_2$ solution without adding oxidizers or inhibitors at 95 °C [203 °F].[14, 16] Crevice corrosion was initiated under open-circuit conditions. Calcium- or magnesium-based chloride solutions can contain more chlorides to be dissolved compared with sodium- or potassium-based solutions. The open-circuit potential decreased after crevice corrosion initiation to values close to the crevice corrosion repassivation potential. The breakdown potential was close to the crevice corrosion repassivation potential. Most crevice sites were corroded. However, the penetration depth was limited, and the deepest penetration was confined to a small area. Sridhar et al.[17] evaluated the behavior of the pitting potential (equivalent to breakdown potential) and the repassivation potential of an analog nickel-based Alloy 825 at 95 °C [203 °F] at various chloride concentrations. At high concentrations of chloride above 1 M, the two potentials merged. This implies that Alloy 22 was easily susceptible to crevice corrosion in 4 M $MgCl_2$ solution without adding oxidizers or inhibitors at 95 °C [203 °F].[16]

Long-Term Crevice Corrosion Tests for 5 Years under Free Corroding Conditions

The Lawrence Livermore National Laboratory conducted crevice corrosion tests of Alloy 22 in simulated concentrated chloride-based ground water solutions using Long-Term Corrosion Test Facility (LTCTF) for maximum approximately 3 years.[18] The solutions were of three types: sodium and potassium derivatives at neutral or slightly basic pH (e.g., simple combination, and about 10 in SCW), sodium and potassium derivatives at low pH (e.g., 2.7 in SAW), and calcium-based solutions. Multi-species solutions such as SAW and SCW also contain various oxyanions, including nitrates, sulfates and bicarbonates. Table 1 presents a summary of the long-term corrosion test cell data. In the table, $\triangle E$ is the difference between repassivation potential and corrosion potential measured (E_{rcrev} - E_{corr}) and was modeled based on the data from these limited tests.

Table 1. Summary of Long-Term Corrosion Test Cell Data[18]

Solution	Immersion Days	Cell #	T(°C)	Creviced Geometry	CC	Rod Geometry	PC	Modeled ΔE		
								Lower Bound	Mean	Upper Bound
5 *m* $CaCl_2$ + 5 *m* $Ca(NO_3)_2$	723	33	120	4	0	2	0	−398	−116	166
5 *m* $CaCl_2$ + 5 *m* $Ca(NO_3)_2$	729	32	100	4	0	2	0	−184	93	370
3.5 *m* NaCl + 0.175 *m* KNO_3 + 0.7 *m* $MgSO_4$	735	31	80	4	2	2	0	−227	38	303
1 *M* NaCl + 0.15 *M* KNO_3	741	30	90	4	0	2	0	−202	62	325
1 *M* NaCl + 0.15 *M* KNO_3	749	29	75	4	0	2	0	−185	80	344
5 *M* $CaCl_2$	650	28	90	4	4	2	0	−466	−201	63
3.5 *m* NaCl + 0.175 *m* KNO_3	252	25	100	4	0	0	0	−225	39	304
3.5 *m* NaCl + 0.525 *m* KNO_3	256	24	100	4	0	0	0	−223	41	305
6 *m* NaCl + 0.9 *m* KNO_3	265	23	100	4	2	0	0	−236	28	291
6 *m* NaCl + 0.3 *m* KNO_3	280	22	100	4	0	0	0	−239	26	290
5 *M* $CaCl_2$ + 0.5 *M* $Ca(NO_3)_2$	463	21	90	6	6	6	0	−597	−332	-66
5 *M* $CaCl_2$	497	20	120	6	6	6	0	−462	−191	79
BSW	256	19	105	0	0	8	0	15	284	554
4 *M* NaCl	328	18	90	0	0	6	0	−233	31	295
SAW w/o Silicate	375	17	90	0	0	6	0	−485	−216	52
SCW	394	16	90	0	0	6	0	124	394	665
5 *M* $CaCl_2$ + 0.5 *M* $Ca(NO_3)_2$	693	15	90	0	0	6	1	−597	−332	−66
5 *M* $CaCl_2$ + 0.05 *M* $Ca(NO_3)_2$	704	14	90	0	0	6	1	−458	−194	70
1 *M* $CaCl_2$ + 1 *M* $Ca(NO_3)_2$	622	13	90	0	0	6	0	−93	186	465
4.5 years LTCTF SAW	834	10	90	0	0	8	0	−435	−168	98
SAW	876	9	90	0	0	8	0	−587	−322	−57
SAW - LTCTF Vessel 26	846	7-2	25	0	0	3	0	−178	106	390
SDW - LTCTF Vessel 30	1,089	6	90	0	0	2	0	18	304	590
SDW - LTCTF Vessel 29	1,089	5	60	0	0	2	0	107	393	678
BSW	729	4	105	1	0	1	0	15	284	554
SCW - LTCTF Vessel 28	1,089	3	90	0	0	2	0	101	373	646
SAW - LTCTF Vessel 26	1,102	2	90	0	0	2	0	−435	−168	98
SAW - LTCTF Vessel 25	1,089	1	60	0	0	2	0	−312	−42	228

Table 1. Summary of Long-Term Corrosion Test Cell Data[18] (Continued)

Solution	Immersion Days	Cell #	T(°C)	Creviced Geometry	CC	Rod Geometry	PC	Modeled ΔE		
								Lower Bound	Mean	Upper Bound
Data below is from cells not used for long-term corrosion potential model development										
1 *m* NaCl + 0.05 *m* KNO_3	223	27	100	4	0	0	0	−218	47	312
1 *m* NaCl + 0.15 *m* KNO_3	230	26	100	4	0	0	0	−217	47	312
5 *M* $CaCl_2$	894	8	120	0	0	5	5	−462	−191	79
SCW - LTCTF Vessel 27	218	7-1	60	0	0	2	0	281	559	837

Source: DTN: LL060900512251.177 [DIRS 178271], file: *Summary Ecorr Cells 1-36 29Sep06.xls*.

Output DTN: MO0703PAGENCOR.001, file: *Ecrit_EcorrValid_Cells3a.xmcd*.

NOTES: Variations in solution composition (e.g., between the SAW solution compositions in Cells, 2, 9, 10, and 17) can lead to variations in the calculated ΔE values. Details of the cell solution compositions can be found in Output DTN: MO0703PAGENCOR.001, file: *EcorrRawData3.xls*.

CC = crevice corrosion, LTCTF = Long-Term Corrosion Test Facility, PC = pitting corrosion, SAW = simulated acidified water, SCW = simulated concentrated water, SDW = simulated dilute water.

As seen in Table 1, many cases demonstrated a negative value of ΔE when the corrosion potential was higher than the repassivation potential. For these negative ΔE values, crevice (or pitting) corrosion is expected from the generally accepted initiation model of crevice corrosion in the literature. However, in the most notable cases of sodium- and potassium-based SAW solution, crevice corrosion was not observed in cells 1, 2, 9, 10 and 17. Furthermore, even many calcium-based solutions did not show crevice corrosion in cells 8, 14, 15, 32, and 33, although 7 out of 17 rods showed pitting corrosion in cells 8, 14 and 15. For concentrated calcium-based solution, crevice corrosion is expected at open-circuit potential, regardless of ΔE value, as inferred from the test in 4 M magnesium chloride solution at 95 °C [203 °F].[16] The breakdown potential was already close to the crevice repassivation potential. Calcium chloride solution is more acidic compared with magnesium chloride solution, and this increases the corrosion potential.

For positive ΔE values when the corrosion potential is lower than the repassivation potential, as expected, all samples were not susceptible to crevice (or pitting) corrosion except two cases in cells 23 and 31. The report[18] explains this exception as model uncertainties in ΔE. As noticed in Table 1, the uncertainties of ΔE values are large. For cell 23, the repassivation potential in a similar solution of 6 M NaCl + 0.3 M KNO_3 at 80 °C [176 °F] was very high, 714 - 682 mV (SSC), and there was very little hysteresis loop in the potentiodynamic polarization. For cell 31, magnesium may have played a role in decreasing the breakdown potential, as discussed above. For both cases, variations of metallurgical conditions of Alloy 22 samples may have contributed to the exception.

Summary of Experimental Data Cited

Under open-circuit corrosion conditions in 5 NaCl solution with 2 x 10^{-4} M $CuCl_2$ at 95 °C [203 °F], stable crevice corrosion was not sustained. The initial corrosion potential was 429 mV (SCE), well above the repassivation potential which was in the range of -145 mV (SCE). In similar tests with $CuCl_2$ at 100 °C [212 °F] at the initial corrosion potential, 260 mV (SCE), the current density was in the passive state. Under open-circuit corrosion conditions in 18 M $CaCl_2$ + 0.9 M $Ca(NO_3)_2$ at 155 °C [311 °F], stable crevice corrosion was not initiated. Most samples showed potential oscillations up to the breakdown potential of 520 – 690 mV (SCE), with respect to the repassivation potential of 31 – 35 mV (SCE). Two samples among five showed pitting outside the crevice. By increasing nitrates, 18 M $CaCl_2$ + 9 M $Ca(NO_3)_2$ at 155 °C [311 °F], crevice corrosion was not initiated and the corrosion potentials were less than the repassivation potential. In more severe environments of 4 M $MgCl_2$ at 95 °C [203 °F] without oxidizers, crevice corrosion was initiated. The corrosion potential was close to the repassivation potential that was in turn close to the breakdown potential as the two potentials merged. In the long-term (maximum 3 years) crevice corrosion tests under free corroding conditions in various chloride solutions at 25 – 120 °C [59 – 248 °F], most samples at corrosion potentials greater than the repassivation potential did not show the initiation of crevice corrosion at 90 - 100 °C [194 – 212 °F]. Exceptions were samples in calcium-based chloride solutions where the corrosion potentials were near to the breakdown potentials.

Model for Cathode Capacity

One of the important factors in the initiation and propogation of the crevice corrosion is the availability of excess cathode current that is generated outside the crevice. The availability of excess cathode current ensures that the electrodes generated due to metal dissolution reaction inside the crevice are actively and instantaneously consumed by the cathode reaction outside the crevice. The cathode capacity is the amount of excess cathode current that balances the metal dissolution current inside the crevice. Shukla, et al.[19] developed a process model to estimate cathode capacity assuming active anodic dissolution of the metal inside the crevice. The following assumptions were made by Shukla, et al.[19] in the model:

- The excess cathode current is generated on the metal surface directly next to a crevice region. Therefore, the electrode potential at the interface of the crevice and open-metal surface is equal to the repassivation potential.

- The oxygen reduction reaction is the dominant cathode reaction within the expected range of the environment.

- The thickness of the brine film on the metal surface is smaller than the length of the film. In addition, the electrolyte conductivity of the brine film is constant.

The model parameters included the difference in corrosion and repassivation potential, kinetic parameters of the oxygen reduction reaction, and length and thickness of the brine films. The model was simulated for various thicknesses of thin film groundwater on the metal surface, length of the water film, and difference between the corrosion and repassivation potential. Figure 5 shows examples of the calculated cathode capacity. When the brine quantity is limited, the rate of oxygen reduction is limited by the electrolyte resistance. As seen in Figure 5, the cathode capacity decreases as the difference between the corrosion and repassivation potential decreases. The horizontal lines in Figure 5 indicate the region where cathode capacity is greater than 10^{-5} A/cm[2.5 x 10^{-5} A/in]. At this level of cathode capacity, a 1 cm^2 of crevice area can be sustained at the corrosion rate of 100 μm/year. The model's results indicate that the difference between corrosion and repassivation potential needs to be at least 0.2 V to sustain a crevice corrosion site as seen in Figure 5 (b).

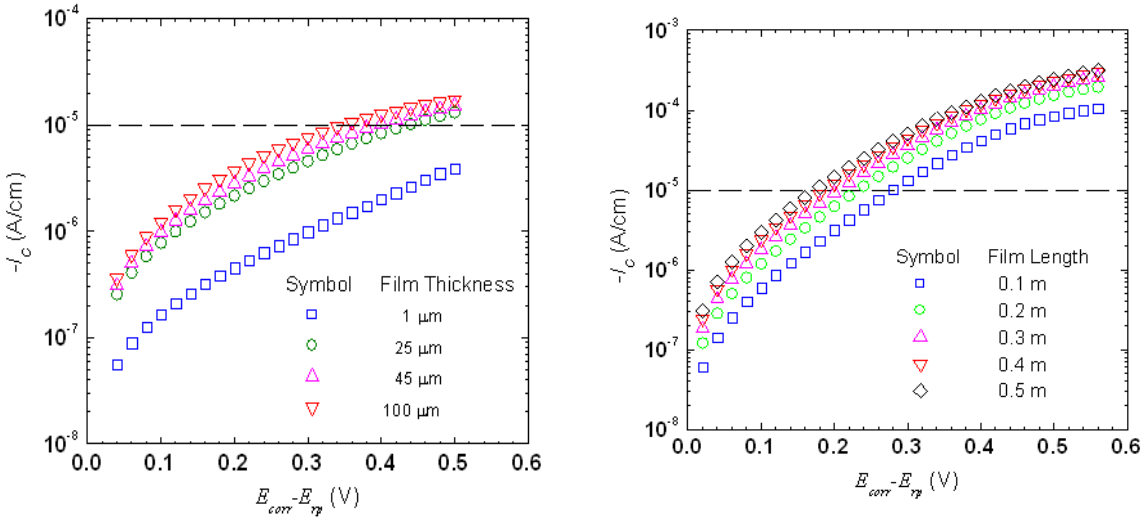

(a) (b)

Figure 5. Calculated cathode capacity of Alloy 22 (a) for constant brine film length, and (b) for constant brine film length as a function of $E_{corr} - E_{rp}$ (i.e., E_{rcrev}) [Shukla, et al.,[19]].

Perspectives on Crevice Corrosion Initiation Criteria

From the "Summary of Experimental Data Cited" and the "Models for Capacity" in sections of this paper, it appears that crevice corrosion of Alloy 22 in concentrated chloride solutions will not be initiated under open-circuit corrosion conditions. To initiate the crevice corrosion under open-circuit corrosion conditions, the corrosion potentials may need to be more anodic toward the breakdown potentials. Currently, the breakdown potentials under open-circuit corrosion conditions are not well defined.

To understand the criteria for crevice corrosion, it is necessary to determine the values of these potentials, including monitoring the corrosion potential continuously with time. Although in the tests and models by Rodriguez, et al.[15] and SNL[18], these values were partially measured, it is unclear whether the repassivation potential and the breakdown potential were measured based on the average current density with time or whether they accurately represented the microstructural characteristics of a localized attack or modification of cathodes. More data may be necessary to define these potentials with time and to generalize the relationship of the localized corrosion and these potentials.

INDUCTION TIMES FOR CREVICE CORROSION

For the long-term prediction of the susceptibility of crevice corrosion, it is necessary to understand whether the measured critical potential in the laboratory, such as the breakdown potential or the repassivation potential, can reasonably represent the long-term behavior of the potentials in the repository. To test this hypothesis, two different types of models pertaining to crevice corrosion initiation were examined.

The first type is a mass transport model to form a steady-state aqueous chemistry inside the crevice. Combrade[11] presented mass transport processes in the crevice for dilute solutions, including diffusion, electrolytic migration, and convection. The author also summarized similar equations using the activity instead of the concentrations developed by Walton.[20] Both models by Combrade[11] and Walton[20] compared the evaluated results of pH and potential inside the crevice, with literature data mainly obtained in the chloride environments. The primary controlling factor was crevice geometry. Given the tight crevice gap and appreciable crevice depth, the pH and potential inside the crevice rapidly dropped with time. The models showed that most cases reached steady-state values of pH and potential within the test period (e.g., 90 hours) except some cases where they continuously decreased at very low rates. Nonetheless, most of the quoted experimental data showed steady-state values within the test time periods. Figure 6 below shows an example case quoted from the work by Walton[20]. As seen in Figure 6, the pH inside the crevice decreases resulting in the increase of the anodic current, indicating more susceptible to localized corrosion when the pH is low. Walton[20] also noted that the steady-state aqueous chemistry inside the crevice could never reach a critical value to initiate crevice corrosion if the ratio of the gap to depth of the crevice is not low enough. The steady-state mass balance inside the crevice depends on this ratio.

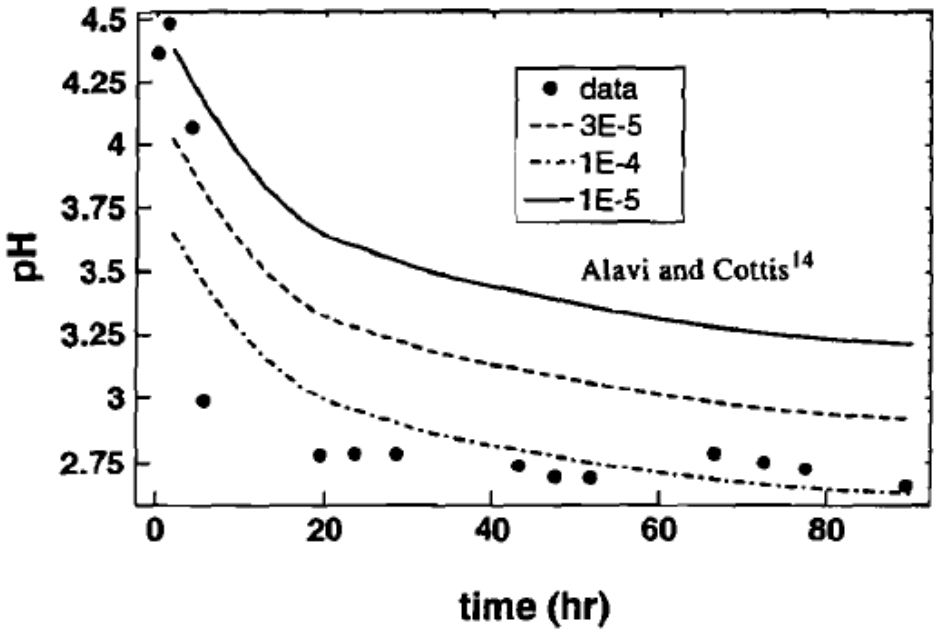

Figure 6. Experimental and Predicted pH values 7.5 cm into the Crevice as a Function of Time Using Different Constant Anodic Current Densities (A/dm^2) [Walton, et al.[20], permission by Elsevier]

A similar observation of the steady-state aqueous chemical behavior inside the crevice was also reported by Shinohara, et al.[21] During the iron dissolution in a crevice in a very dilute sodium sulfate or sodium chloride solution, the steady-state current-time transient arrived in ~ 11 hours. Currently, the coauthors of this paper by Shinohra, et al.[21] are

conducting similar modeling as shown in Figure 6. The efforts consider nickel-based alloys including Alloy 22.

Once the steady-state chemistry, pH and potential are maintained inside the crevice, it may still take time to initiate rapid crevice corrosion inside the crevice. The crevice corrosion normally propagates in the form of pitting in a steady-state,[14,16] although it may look to propagate more uniformly as passivity breaks down at low magnification in the beginning. The inside crevice surface is of heterogeneous geometry, and not smooth microscopically.[6,11] Therefore, it has been postulated that micro electrochemical cells will form inside the crevice, and the microcell formation could propagate the crevice corrosion in more localized micro form, i.e., pitting [Figure 3, Payer and Kelly;[6] or Figures 22 and 23, Combrade[11]]. Since pitting is the most likely form in the localized corrosion inside the crevice as observed, it is worth examining a model for the induction time for pitting.

Lin, et al.[1] and Urquidi-Macdonald and Macdonald[22] developed models for the induction times for pitting corrosion of passive iron or carbon steel in borate buffer solution by varying chloride concentrations and pH at 25 °C [77 °F]. Equation 1 and Figure 7 below present the results.

The induction time is

$$t_{ind} = \varepsilon \, [\exp \{\chi \, F \, \alpha \Delta V)/(2 \, R \, T)\} - 1]^{-1} + \xi \qquad (1)$$

where ε is a function of chloride activity, critical potential, diffusivity of cation vacancy, and a critical amount of metal holes; χ is the charge on a cation; F is the Faraday constant; α is a constant relating to the potential drop at the film/solution interface; ΔV is applied potential minus the critical potential (pitting potential or breakdown potential); R is the gas constant; T is temperature; and ξ is transient aqueous diffusion time.

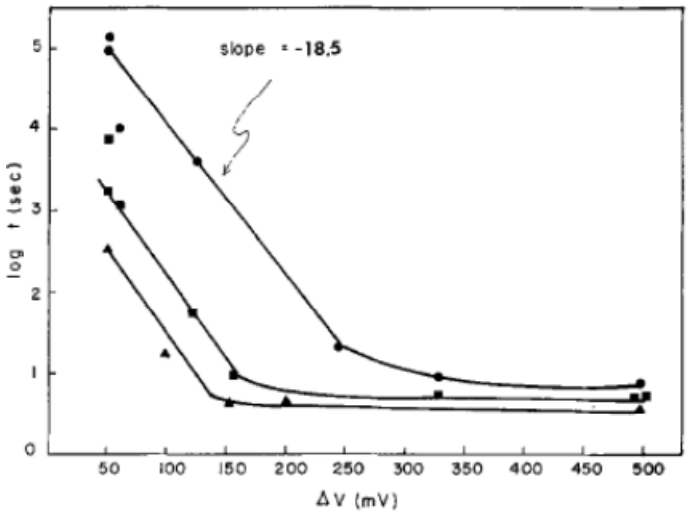

Figure 7. Induction Time vs. ΔV
Data for Pitting of Passive iron in Borate Buffer Solution at 25 °C [77 °F]. Triangle: pH 7.3 0.1 M NaCl, Rectangle: pH 7.3 0.01 M NaCl, Circle: pH 8.3 0.01 M NaCl [Lin, et al.,[1] permission by The Electrochemical Society]

The equation for induction time, t_{ind}, above, and its distribution discussed below were based on the point defect model (PDM) of passive film of carbon steel and passive iron. This induction time is an exponentially sensitive function of Δ V (applied potential or corrosion potential minus the critical potential such as breakdown potential). According to PDM, the excess amount of cation vacancies form voids at the metal-oxide interface in the p-type passive oxide film as observed in the case of carbon steel in 0.8 M NaCl + 0.1 M $CuCl_2$ solutions at 250 °C [482 °F].[23]

The PDM was also adopted to explain the passivity breakdown of Alloy 22 corroded in saturated NaCl solutions at 80 °C [176 °F].[24] In the range of potentials close to the film breakdown potential, ~ 600 mV (SHE), the anodic current increased sharply and the oxide film changed to p-type semiconductor from n-type semiconductor. Above the breakdown potential, Alloy 22 showed transpassive dissolution, and Macdonald, et al.[24] postulated that the passive film could break down due to the generation of excess cation vacancies via the oxidative ejection of Cr(VI) species from the barrier layer, resulting in film breakdown. Alternatively, if Alloy 22 passive film remains as n-type semiconductor with charge carrier of oxygen vacancy, a similar formula could be obtained regardless of the nature of semiconducting properties of oxide.[25] Lin, et al.[1] derived the induction time by balancing vacancy flux and its sink at the interface of metal-oxide interface [Equation 3 of Lin, et al.[1]]. When the balance results in forming the critical size of void by condensing vacancies, the passivity will break down. The driving force for the vacancy condensation is applied (or corrosion) potentials which are exponentially related to the flux. The sharp rapid decrease of induction times with driving force for nucleation is typical in many solid-state nucleation processes.[26,27]

Recent publications by Macdonald and his coworkers provide parameter values in the PDM model applied to Alloy 22.[25,28] For example, the steady-state passive current density and the steady-state thickness of passive film were of very similar forms as the original forms developed for steel, iron and nickel.[23,25,29,30] The evaluated steady-state thickness of passive film was in the range of that in steel and iron. The detailed formulation and evaluation of the induction and its distribution for Alloy 22 have not been conducted here and are beyond the scope of this work. Therefore, this paper highlights only the functional behavior of the equation in Figure 7 with time.

When the applied potential (or corrosion potential) reaches the theoretical critical potential (in this case the breakdown potential), $\triangle V \sim 0$, the induction time becomes infinite in Equation (1). This infinite induction time is also shown in the plot of calculated values at the left end of the X axis [ΔV (mV) ~ 0] in Figure 7. If the applied potential (or corrosion potential) exceeds the critical potential by as low as ~50 mV, the induction time becomes short enough to be determined in the laboratory tests as shown in Figure 7. The ~ 50 mV in this case could be within the measurement uncertainty limit in the measurement of long-term corrosion potential [see more explanations in Ahn, et al.[31]]. Some example cases of the fluctuation in long-term corrosion potentials with time as long as about three years are in Figures 6-35 and 6-37 of SNL[18]. These figures indicate that the induction times observed in the laboratory measurements are the maximum values. Therefore, given the external environmental conditions, metallurgical conditions of Alloy 22, and the crevice geometry, extremely long induction times beyond laboratory tests are unlikely to exist.

Urquidi-macdonald and Macdonald[22] formulated the distribution of the critical potential (and the corresponding distribution of induction time) based on PDM.[1] Increasing the distributed induction time from the average induction time of 100 seconds to ~ one year, the frequency of pitting decreased to be negligible in the case of example calculation for the system of Fe-17Cr in 3.5% NaCl solution at 30 °C [86 °F].[31] In the experiments of Alloy 22 in 4 M MgCl at 110 °C [230 °F] and in 5 M NaCl solution at 95 °C [203°F],[14,16] similar behavior of the decreased frequency was observed. The pit density inside the crevice decreased gradually with time, as discussed in the previous section with respect to the breakdown potential for pit initiation. The decreased frequency of pitting with time again implies that extremely long induction time beyond laboratory tests are unlikely to exist because no long-term latent pitting is expected.

Even in the potentiostatically determined repassivation potential for the initiation of crevice corrosion of Alloy 22, a similar sharp dependence of initiation time for the crevice corrosion was observed. With existing pit or crevice corrosion, the repassivation time was measured by increasing the applied potential from the potential well below the repassivation potential. The repassivation time of the intentionally created pits was short with increasing potential until very near to the repassivation potential where the repassivation times increased sharply for a very long time.[32] In this case too, it appears that the repassivation process involved a solid-state nucleation process (e.g., oxide reformation[33]) that has typically such a sharp dependence of the induction time on the driving force for nucleation (e.g., the applied potential).

Theoretical models were evaluated for electrochemical induction times for pitting corrosion (possibly inside the crevice) and for mass transport kinetics for crevice corrosion. In both cases, the long-term steady states can be reached in the laboratory time scale, because the induction times are short within the uncertainties of the measurements.

SUMMARY

1. The electrochemical criteria for the initiation of crevice corrosion of Alloy 22 in concentrated chloride solutions at near-boiling temperatures were reviewed and evaluated. The applicability of the laboratory-measured repassivation and breakdown potential as a criteria for the initiation of crevice corrosion was evaluated for its use in a very long period of time of the conservative-based performance assessment of nuclear waste management.

2. With externally applied current between the anode and the cathode of a crevice cell, crevice corrosion may be initiated at the corrosion potential above the repassivation potential. Under the free corroding conditions, however, crevice corrosion may not be initiated even in the long term at the corrosion potential above the repassivation potential until the corrosion potential reaches a breakdown potential. Various laboratory data obtained from tests under open-circuit or free corroding conditions as long as 3 years support this hypothesis. Models for the modification of cathode capacity with time also support this hypothesis. More data may be necessary to generalize this hypothesis by reducing the associated uncertainties, and the breakdown potential needs to be better defined especially under open-circuit or free corroding conditions.

3. Models for the induction times for crevice corrosion were evaluated to assess whether laboratory tests could represent the very long-term crevice corrosion behavior. It appears that data on the initiation time for crevice corrosion measured in the laboratory time scale may be suitable to represent performance for a very long period of time, given the environmental or metallurgical conditions.

REFERENCES

1. L. F. Lin, C. Y. Chao and D. D. Macdonald, A Point Defect Model for Anodic Passive Films, II. Chemical Breakdown and Pit Initiation, J. Electrochemical Society, Vol.128, p. 1194, 1981

2. D. S. Dunn, O. Pensado, Y.-M. Pan, R. T. Pabalan, L. Yang, X. He and K. T. Chiang, Passive and Localized Corrosion of Alloy 22–Modeling and Experiments, CNWRA 2005-02, Rev. 1, Center for Nuclear Waste Regulatory Analyses, San Antonio, TX, 2005

3. Sandia National Laboratories (SNL), "Total System Performance Assessment Model/Analysis for the License Application," MDL-WIS-PA-000005 REV 00 ADD 01 ERD 3, Las Vegas, Nevada, 2008

4. X. Shan and J. H. Payer, Effect of Crevice Former on the Evolution of Crevice Damage, CORROSION 2008 CONFERENCS & EXPO, Paper No. 08575, NACE International, Houston, TX, 2008

5. R. M. Carranza, The Crevice Corrosion of Alloy 22 in the Yucca Mountain Nuclear Waste Repository, J. of Metals, Vol. 60, pp. 58-65, 2008

6. J. H. Payer and R. G. Kelly, Perspectives on Localized Corrosion in Thin Layers of Particulate, Mat. Res. Soc. Symp. Proc. Vol. 985, pp. 237-248, 2007

7. R. M. Carranza, M. A. Rodríguez and R. B. Rebak, Environmental and Geometrical Conditions to Sustain Crevice Corrosion in Alloy 22, CORROSION 2007 CONFERENCES & EXPO, Paper No. 07581, NACE International, Houston, TX, 2007

8. A. Yilmaz, P. Pasupathi and R. B. Rebak, Stifling of Crevice Corrosion in Alloy 22 during Constant Potential Tests, American Society of Mechanical Engineers, Pressure Vessels and Piping Division (Publication) PVP, Vol. 7, pp. 493-502, 2005, Proceedings of the ASME Pressure Vessels and Piping Conference 2005 – Operations, Applications and Components, PVP2005

9. R. B. Rebak, Factors Affecting the Crevice Corrosion Susceptibility of Alloy 22, CORROSION 2005, Paper No. 05610, NACE International, Houston, TX, 2005

10. N. S. Meck, P. Crook, S. D. Day and R. B. Rebak, Localized Corrosion Susceptibility of Nickel Alloys in Halide Containing Environments, CORROSION 2003, Paper No. 03682, NACE International, Houston, TX, 2003

11. P. Combrade, The Crevice Corrosion of Metallic Materials, Chapter 11 in *Corrosion Mechanisms in Theory and Practice*, second edition, edited by Ph. Marcus, Marcel Dekker, Inc., NY, pp. 349 – 397, 2002

12. Z. Szklarska-Smialowsak, *Pitting Corrosion of Metals*, National Association of Corrosion Engineers, Houston, TX, 1986

13. ASM International, ASM Handbook, Formally Ninth Edition, Metals Handbook, Volume 13. Corrosion, 1987

14. X. He and D. S. Dunn, Crevice Corrosion Penetration of Alloy 22 in Chloride-Containing Waters–Progress Report, CNWRA 2006-001, Center for Nuclear Waste Regulatory Analyses, San Antonio, TX, 2005

15. M. Rodriguez, M. Stuart and R. Rebak Long Term Electrochemical Behavior of Creviced and Non-Creviced Alloy 22 in CaCl2 + Ca(NO3)2 Brines at 155 EC, CORROSION 2007 CONFERENCES & EXPO, Paper No. 07577, NACE International, Houston, TX, 2007

16. X. He and D. S. Dunn, Crevice Corrosion Propagation Behavior of Alloy 22 in Extreme Environments, CORROSION 2007 CONFERENCES & EXPO, Paper No. 07578, NACE International, Houston, TX, 2007

17. N. Sridhar, G. Cragnolino and D. Dunn, Experimental Investigations of Failure Processes of High-Level Radioactive Waste Container Materials, CNWRA 95-010, Center for Nuclear Waste Regulatory Analyses, San Antonio, TX, 1995

18. SNL, General Corrosion and Localized Corrosion of Waste Package Outer Barrier, ANL-EBS-MD-000003 REV 03 CAN 01 ERD 1, Las Vegas: Sandia National Laboratories, 2007

19. P. K. Shukla, R. Pabalan, T. Ahn, L. Yang, X. He and H. Jung, Cathode Capacity of Alloy 22 in the Potential Yucca Mountain Repository Environment, CORROSION 2008, New Orleans, Louisiana, U.S. Nuclear Regulatory Commission ADAMS ML080630670, 2008

20. J. C. Walton, G. Cragnolino and S. K. Kalandros, A Numerical Model of Crevice Corrosion for Passive and Active Metals, Corrosion Science, Vol. 38, No. 1, pp. 1 – 18, 1996

21. T. Shinohara, S. Fujimoto, N. J. Laycock, A. Msallem, H. Ezuber and R. C. Newman, Numerical and Experimental Simulation of Iron Dissolution in a Crevice with a Very Dilute Bulk Solution, J. Electrochemical Soc., Vol. 144, p. 3791, 1997

22. M. Urquidi-Macdonald and D. D. Macdonald, Theoretical Distribution Functions for the Breakdown of Passive Films, J. Electrochemical Society, Vol. 134, P. 41, 1987

23. D. D. Macdonald, The Point Defect Model for the Passive State, J. Electrochemical Society, Vol. 139, pp. 3434 - 3448, 1992.

24. D. D. Macdonald, A. Sun, N. Priyantha, and P. Jayaweera, An Electrochemical Study of Alloy 22 in NaCl Brine at Elevated Temperature: II. Reaction Mechanism Analysis, J. Electroanalytical Chemistry, Vol. 572, P. 421, 2004

25. D. D. Macdonald, On the Tenuous Nature of Passivity and its Role in the Isolation of HLNW, J. Nuclear Materials, Vol. 379, pp. 24 – 32, 2008

26. T. Ahn, Dry Oxidation and Fracture of LWR Spent-Fuels, NUREG-1566, U.S. Nuclear Regulatory Commission, Washington, D.C., 1996

27. V. Christian, The Theory of Transformation in Metals and Alloys, Part I, "Equilibrium and General Kinetic Theory," Second Edition, Pergamon Press, New York, NY, 1975

28. L. G. McMillion, D. A. Sun, D. D. Macdonald and D. A. Jones, General Corrosion of Alloy 22: Experimental Determination of Model Parameters from Electrochemical Impedance Spectroscopy Data, Met. Mat. Transactions A, Vol. 36A, pp. 1129 – 1141, 2005

29. D. D. Macdonald, S. R. Biaggio and H. Song, Steady-State Passive Film, J. Electrochemical Society, Vol. 139, pp. 170 – 177, 1992

30. D. D. Macdonald and M. Urquid-Macdonald, Theory of Steady-State Passive Film, J. Electrochemical Society, Vol. 137, pp. 2395 – 2403, 1990

31. T. Ahn, H. Jung, X. He and O. Pensado, Understanding Long-Term Corrosion of Alloy 22 Container in the Potential Yucca Mountain Repository for High-Level Nuclear Waste Disposal, J. Nuclear Materials, Vol. 379, pp. 33 – 41, 2008

32. D. S. Dunn, G. A. Cragnolino and N. Sridhar, Long-Term Prediction of Localized Corrosion of Alloy 825 in High-Level Nuclear Waste Repository Environments, Corrosion, Vol. 52, p. 115, 1996

33. T. Okada, Halide Nuclei Theory of Pit Initiation in Passive Metals, J. Electrochemical Society, Vol. 131, p. 241, 1984

Disclaimer

The NRC staff views expressed herein are preliminary and do not constitute a final judgment or determination of the matters addressed.